Dalton Transactions

ROYAL SOCIETY OF CHEMISTRY

PAPER

View Article Online
View Journal | View Issue

Check for updates

Cite this: *Dalton Trans.*, 2024, **53**, 13065

Adsorbents for hydrogen-bond accepting hazardous chemicals by post-synthetic modification of UiO-66-NH_2†

Daniel A. Corbin, [a] Michael R. Papantonakis,[b] Viet K. Nguyen,[b] Christopher J. Breshike*[b] and R. Andrew McGill[b]

Received 15th April 2024,
Accepted 3rd July 2024

DOI: 10.1039/d4dt01113a

rsc.li/dalton

Adsorbents for hydrogen-bond accepting chemicals such as organophosphates are developed by post-synthetically modifying UiO-66-NH_2 through two analogous condensation reactions to incorporate hydrogen-bond donating adsorbent groups. When benzaldehydes are employed as coupling partners, the resulting imine-functionalized MOFs show improvements in uptake capacity with increasingly electron-deficient adsorbent groups. By contrast, when the coupling partners are benzoic acids, the resulting amide-functionalized MOFs exhibit improvements in uptake capacity with increasingly electron-rich adsorbent groups. Both modification approaches also increase binding affinity for organophosphates relative to unmodified UiO-66-NH_2, demonstrating successful modification of the MOF scaffold to create adsorbents for hazardous chemicals.

Introduction

Sorbents are a critical component of protection/detection technologies employed by military personnel and first responders to remove and identify toxic chemicals in air.[1,2] One common sorbent is activated carbon, which is often used for the broad protection it provides against a wide array of chemicals.[2–4] This sorbent material has found numerous applications in protection technologies dating back to World War I, and methods have been developed over time to improve upon its performance. One example includes impregnating the activated carbon with metals such as copper, silver, zinc, and molybdenum, as well as organic molecules such as triethylenediamine (TEDA). This formulation is known as ASZM-TEDA carbon, and it is commonly used in military-grade gas mask filters.[2]

Despite the popularity of activated carbon sorbents, they suffer from several limitations. For example, activated carbon struggles to capture small, highly polar molecules such as ammonia, limiting its utility in certain applications. In these instances, impregnated materials must be used to effectively capture the target chemical.[5] In addition, the performance of activated carbons suffers at high relative humidity,[3,6] making its use in certain operational environments challenging. From a research perspective, the structures of these materials are also poorly defined and irregular, so systematic investigations to improve their performance can be challenging.[4]

Another class of polymeric sorbent materials has been developed as preconcentrators for detection applications, where a thin coating of the sorbent is applied to a sensor to increase its selectivity and sensitivity for certain target chemicals. Early work in this area led to the development of fluoropolyol (FPOL, Fig. 1),[7] a fluorinated polymer that later found

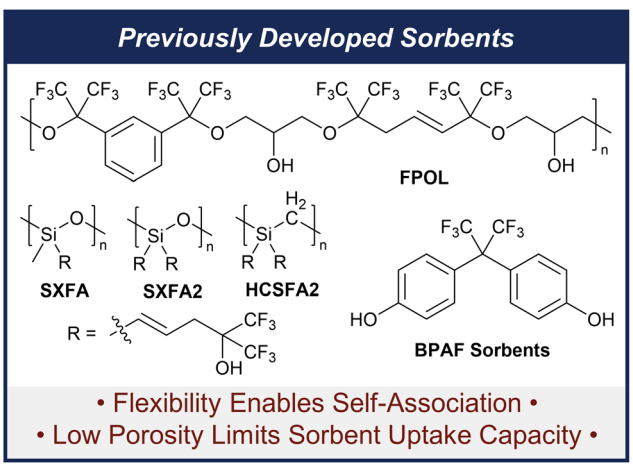

Fig. 1 Previous polymeric and small molecules sorbents developed for detection applications.

[a]*National Research Council Research Associateship Program, Washington, DC 20375, USA*
[b]*Materials and Sensors Section, US Naval Research Laboratory, 4555 Overlook Ave SW, Washington, DC 20375, USA. E-mail: christopher.j.breshike.civ@us.navy.mil*
†Electronic supplementary information (ESI) available. See DOI: https://doi.org/10.1039/d4dt01113a

application in surface acoustic wave sensors for the detection of organophosphate chemicals.[8–11] More recently, our group reported on the development of several silicon-based polymers for preconcentrator applications,[12,13] as well as small molecule sorbents based on bisphenol A for organophosphate detection (Fig. 1).[14,15] While these materials are useful for detection, their use in protection technologies is limited by their non-porous nature, which severely limits their uptake capacity and adsorption kinetics. Further, all of these polymeric and small molecule sorbents suffer from self-association interactions, in which the hydroxyl groups responsible for binding the target chemical hydrogen-bond with each other instead, creating competition for binding sites within the sorbent.[15] To overcome these issues, we wondered whether it might be possible to graft similar functionalities for organophosphate capture within a metal–organic framework (MOF) scaffold to achieve a sorbent that is porous, rigid, and selective (Fig. 2).

A lot of work has been done using MOFs for organophosphate removal both as adsorbents[2–4,16,17] and catalysts[16,18] for degradation. Ni *et al.* reported on the use of IRMOF-1 for the capture of dimethyl methylphosphonate (DMMP).[19] Later, Britt *et al.* demonstrated that MOFs can even outperform activated carbons in certain gas adsorption applications by investigating a series of isoreticular MOFs in the presence of several hazardous chemicals, including ammonia, benzene, and sulfur dioxide.[20] However, many of these early MOF adsorbents exhibited poor stability under ambient conditions,[19] a property that was attributed to hydrolysis of the metal–oxide bonds connecting the metal nodes of the MOFs to the organic linkers. To overcome this issue, hydrophobic MOFs were designed to adsorb target chemicals while avoiding undesirable interactions with water.[21–23] Another approach involved inserting sorbent functional groups within a MOF with greater chemical stability, such as a zirconium MOF with carboxylate linkers.[16,24,25]

This work utilizes the latter approach of post-synthetic modification. Since the chemical stability of UiO-66 MOFs has been well established,[26] this MOF series was chosen for post-synthetic modification (PSM) to install the desired adsorbent moieties for organophosphate capture within a chemically robust and porous scaffold. Following confirmation of MOF functionalization, the properties of these MOF-based adsorbents were probed in a series of adsorption experiments with DMMP, a common organophosphate simulant used in vapor-phase studies.[2–4,8,11,13,15,19] Through these investigations, design principles were identified to guide future work in this area.

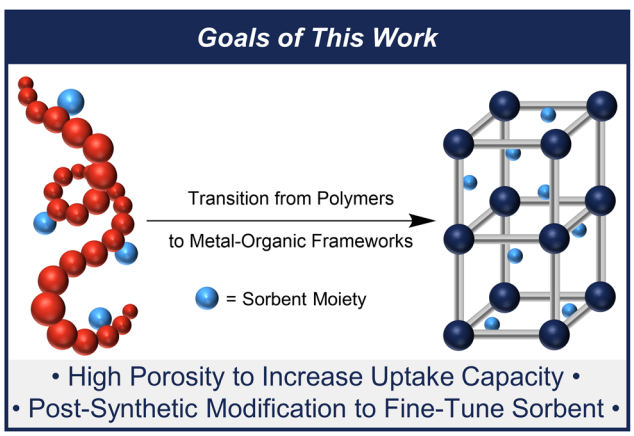

Fig. 2 The goal of this work is to develop tunable adsorbents by post-synthetic modification of MOFs.

Experimental

Chemical sources and storage

Unless otherwise noted, all reagents were obtained from either Sigma Aldrich or Ambeed and used as received. All manipulations were carried out in a standard laboratory fume hood under ambient atmosphere. MOFs were stored under ambient conditions and dried thoroughly prior to analysis by drying overnight at 120 or 200 °C under reduced pressure.

General procedure for MOF functionalization

UiO-66, UiO-66-OH, and UiO-66-NH_2 were synthetized according to a literature procedure.[27] A single batch of UiO-66-NH_2 was synthesized and used for all subsequent modifications to eliminate batch-to-batch variations that might influence adsorbent performance.

UiO-66-NH_2 was functionalized according to modified literature procedures.[28–30] UiO-66-NH_2 (200 mg) was weighed into a 20 mL glass scintillation vial. The quantity of amine-groups in this amount of UiO-66-NH_2 was approximated based on the mass-ratio of $-NH_2$ to an ideal MOF formula unit [$Zr_6O_4(OH)_4$(BDC-NH_2)$_6$], where [BDC-NH_2 = 2-amino-1,4-benzenedicarboxylate]. The mass of $-NH_2$ in 200 mg of UiO-66-NH_2 was then converted to moles (0.684 mmol, 1 eq.). For each functionalization reaction, the chosen coupling partner was weighed and added to the reaction vial (1.368 mmol, 2 eq.), along with methanol (10 mL) and a magnetic stir-bar. The reaction was stirred at room temperature for 7 days, after which the product was collected by vacuum filtration and washed with clean methanol (4 × 10 mL). The product was dried briefly under air before being left to dry further in a vacuum oven at 120 °C for several days.

In some cases, residual coupling partner in the functionalized MOF could be observed by ^{1}H NMR after suspending the MOF in D_2O for 30 minutes. For each sample where this impurity was found, the functionalized MOF was soaked in methanol overnight, filtered, and dried again as described above. In most cases, this procedure was sufficient to remove all detectable residual coupling partner.

General procedure for MOF digestion

MOF digestion using sodium bicarbonate was performed according to a modified literature procedure.[31] A small quantity of MOF (~2–5 mg) was added to an NMR tube along with 0.4 mL of saturated $NaHCO_3$ in D_2O. The solution was mixed

vigorously and allowed to react for 30 minutes. In most cases, the solution changed from colorless to lightly colored (typically yellow or orange), and some solid remained in the bottom of the NMR tube. The solution was immediately characterized by NMR spectroscopy.

General procedure for imine MOF reduction

A small quantity of MOF (~5 mg) was added to a 2 mL glass scintillation vial and suspended in ethanol (0.5 mL). The vial was sonicated for a few minutes to fully suspend the solid. A photograph of the suspension was taken prior to addition of a reducing agent for future comparison, and excess sodium borohydride was added to the suspension along with a magnetic stir bar. The reaction was stirred for 24 h, during which the color of the suspension gradually became lighter. After 24 h, a second photograph of the suspension was taken to record the change in color and compare to the pre-reaction photograph.

Results and discussion

The UiO-66 series of MOFs was selected for its excellent stability in both humid and chemical environments.[26] UiO-66 was selected as a control system for these studies, as it lacks a binding site specifically designed for adsorption of hydrogen-bond accepting chemicals. UiO-66-OH was also selected for control studies, since every linker contains a hydroxyl group capable of hydrogen-bonding with the target chemicals. For incorporation of adsorbent groups, UiO-66-NH_2 was selected given the vast array of modifications reported for the amino-functionalized linkers within this MOF.[28–30,32–38] In each case, UiO-66 series MOFs were synthesized using the procedure reported by Katz *et al.* with hydrochloric acid as a mediator,[27] and all UiO-66-NH_2 used in this investigation was synthesized in a single batch to avoid batch-to-batch variability.

To target hydrogen-bond accepting adsorbates such as organophosphates, UiO-66-NH_2 was modified to incorporate hydroxyl groups that can act as hydrogen-bond donating groups. In our previous work, it was observed that further functionalizing sorbents with electron-withdrawing groups could increase binding affinity for organophosphates by increasing the acidity of the sorbent hydroxyl group.[15] As such, in this work we sought to incorporate groups with tunable electronics to better understand how this property impacts sorbent performance. Specifically, we targeted phenolic groups with *ortho*- and *meta*-substituents that could be varied from electron donating (OMe) to withdrawing (F and CF_3) in nature (Fig. 3).

Functionalization of UiO-66-NH_2 was achieved using modified literature procedures for the condensation of benzaldehydes[28,29] and benzoic acids[30] with the amine-functionalized linkers. In reactions with benzaldehydes (the *imine series*, Fig. 3, left), the imine bridges formed between the linkers and the adsorbent groups give rise to extended conjugation within the MOF, resulting in a characteristic yellow-orange color.[28,29] Instead, reactions with benzoic acids (the *amide series*, Fig. 3, right) result in the formation of an amide bridge that does not alter the conjugation of the system. As a result, little-to-no color change is observed for amide-functionalized MOFs, giving them a similar appearance to UiO-66-NH_2.[30] In both cases, methanol was selected as the reaction solvent to ensure solubility of the starting materials.

In an effort to verify functionalization of the MOFs, characterization was performed by nuclear magnetic resonance (NMR) spectroscopy on samples digested using saturated

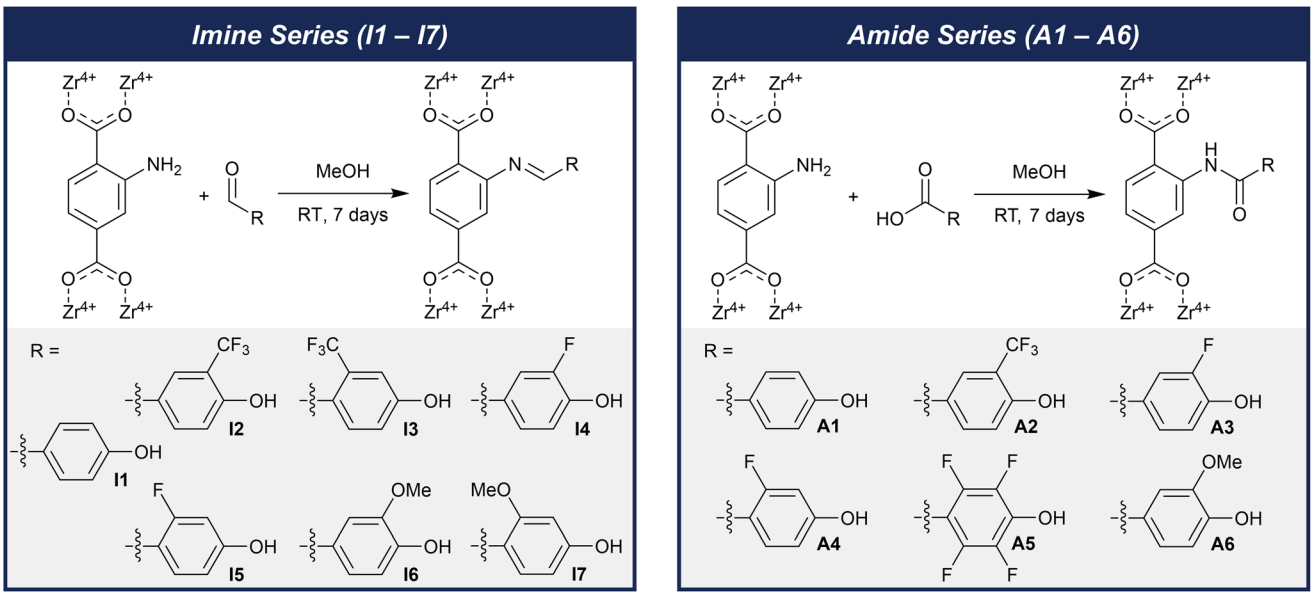

Fig. 3 Reactions employing benzaldehyde (left) and benzoic acid (right) coupling partners to generate imine- and amide-functionalized MOFs, respectively.

sodium bicarbonate in D_2O.[31] While digestion of UiO-66 MOFs is typically performed using hydrofluoric acid solutions,[34,36,38,39] this approach was avoided out of concern that the acidic digestion solution would likely hydrolyze the imine- and amide-bridging groups.[40] Upon digestion of the functionalized MOFs, the resulting NMR spectra were compared to digested UiO-66-NH_2 and the respective coupling partner under the same conditions (sat. $NaHCO_3$ in D_2O). An example of this data is provided in Fig. 4 for **I7**, which exhibits signals corresponding to both the linker and the benzaldehyde coupling partner used in the synthesis of **I7**. However, minimal, if any, peak shifts are observed between the starting materials and the functionalized MOF, suggesting the observed spectrum for digested **I7** is a mixture of the UiO-66-NH_2 linker and the benzaldehyde coupling partner.

Since imine hydrolysis can also be catalyzed by base,[41] it is possible that even the weak-basic conditions in the $NaHCO_3$ digestion cause hydrolysis of the imine group to reform the NH_2-linker and benzaldehyde coupling partner. However, one cannot discount the possibility that that functionalization was unsuccessful, and that the coupling partner was simply intercalated into the MOF rather than covalently bound. To test this alterative hypothesis, each functionalized MOF was soaked in D_2O, and the supernatant was analyzed again by NMR spectroscopy to search for free coupling partner diffusing out of the MOF. In nearly every case, no free coupling partner was observed (Fig. S17–S53†).

In addition, a small molecule model reaction was carried out for **I6** by reacting vanillin (4-hydroxy-3-methoxybenzaldehyde) with dimethyl aminoterephthalate. Immediately, a color change from colorless to yellow-orange was observed (Fig. S56†), similar to the color changes observed for the Imine series f-MOFs. The product of this reaction was then analyzed by NMR spectroscopy in several solvents. In deuterated chloroform, several shifted signals were observed relative to the starting materials (Fig. S55 and S56†), and integration of the product spectrum was consistent with formation of the desired coupling product. However, when analysis in D_2O was attempted, the product appeared to undergo hydrolysis to yield a mixture of vanillin and dimethyl aminoterephthalate. Only signals corresponding to vanillin could be observed, while the dimethyl aminoterephthalate signals were not seen, likely due to the poor solubility of this compound in D_2O (Fig. S57†). As such, we propose these results are consistent with successful functionalization of UiO-66-NH_2 with imine functional groups, which undergo hydrolysis in the aqueous conditions used for MOF digestion.

Further support for the formation of these bridging groups was sought through UV-visible (UV-vis) spectroscopy to probe for the presence of the expected imine. Recent work functionalizing UiO-68 derivatives with imine groups showed similar color changes for the MOFs upon functionalization, as well the formation of new spectroscopic features in their UV-vis spectra stemming from the imine groups.[42] As such, the UV-vis spectra of the functionalized MOFs in this work were also collected (Fig. 5). The best results were obtained for suspensions prepared in DMF and sonicated to disperse the solid particles prior to measurement. However, only one of the samples (**I7**) showed the expected shoulder around 450 nm corresponding to the imine. This result is surprising given that all the functionalized MOFs are visually darker in color than unmodified UiO-66-NH_2 (Fig. 5). However, it is possible that the expected spectroscopic feature is obscured in the UV-vis spectra due to scattering of the source light and the low degree of functionalization for some of the materials (see below). Notably, a similar feature was observed for the small molecule analogue of **I6** (Fig. S58 and S59†), supporting the assignment of this absorption signal to the imine functional group.

In an effort to demonstrate that the color changes observed for **I1–I7** are indeed due to the presence of the imine bridges, the imine was reduced to an amine and monitored for the disappearance of the MOF's yellow-orange color. Reduction of the imine-functionalized MOF **I7** was carried out using excess sodium borohydride[42] in ethanol and monitored over 24 h. The expected loss of color was observed (Fig. 6), supporting the presence of an imine group within these materials. Further confirmation was obtained by repeating this experiment for **I6**, which does not show UV-vis spectroscopic evidence of an imine but does exhibit a similar yellow-orange color to **I7**. Again, treatment with sodium borohydride resulted in loss of color over 24 h (Fig. S61†). Further, digestion and ^1H NMR analysis of this reduced material showed disappearance of the assigned imine signal at 9.37 ppm (Fig. S62†), supporting the presence of an imine bond in **I6**. Taken together, these data suggest that the adsorbent groups are incorporated through covalent bonds, but that these bonds are susceptible to hydro-

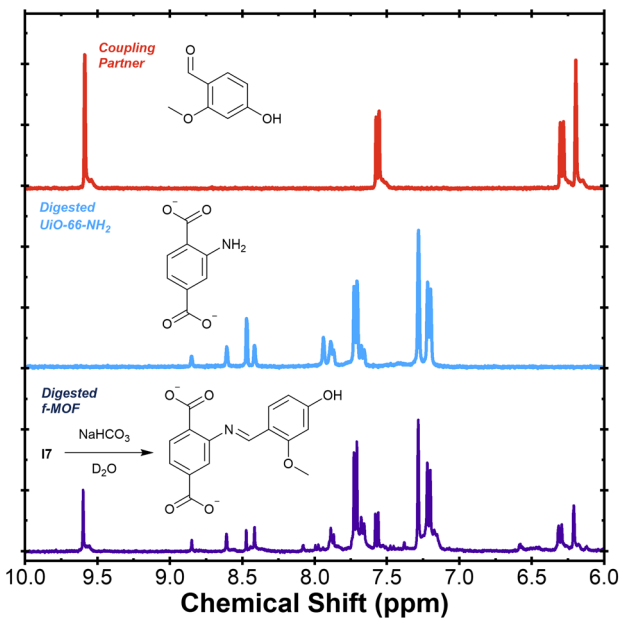

Fig. 4 Digestion of **I7** in saturated $NaHCO_3$ and its resulting ^1H NMR spectra (bottom, dark blue). The spectra of digested UiO-66-NH_2 (middle, light blue) and the benzaldehyde coupling partner in the presence of sat. $NaHCO_3$ (top, red) are provided for reference.

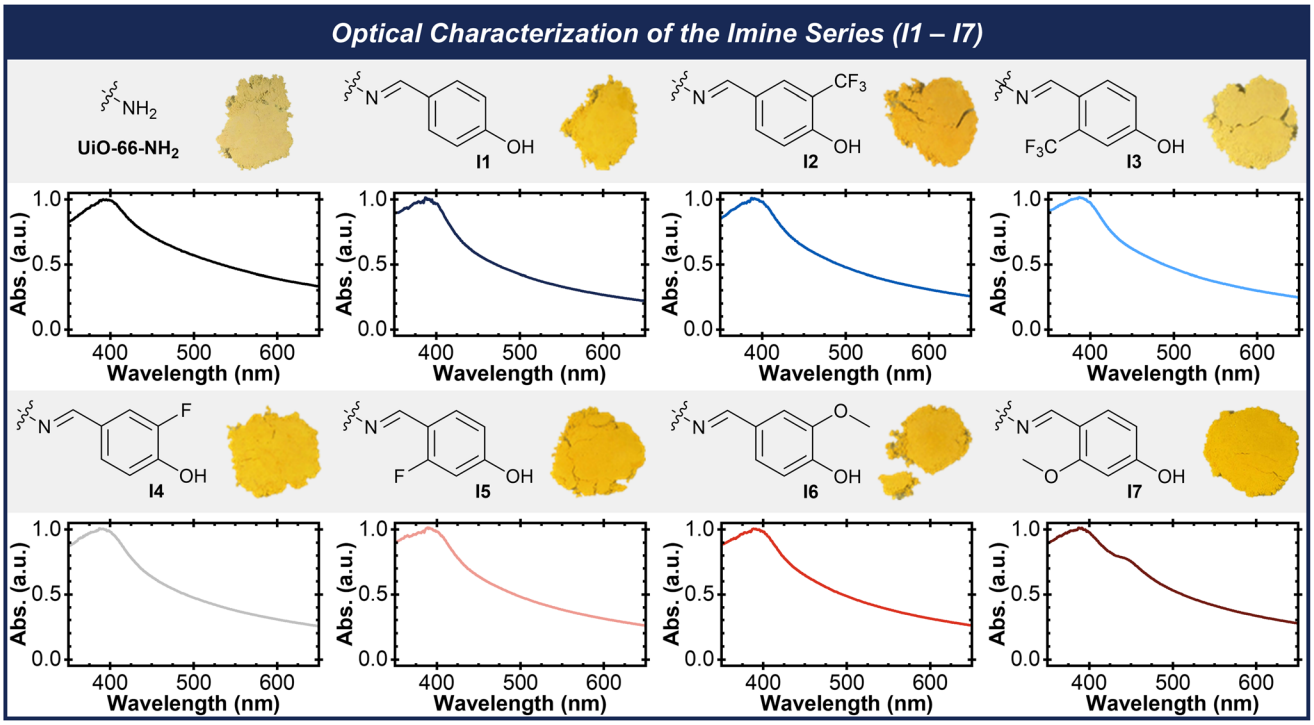

Fig. 5 Photographs of imine-functionalized MOFs **I1–I7** and normalized UV-vis spectra of their suspensions in DMF. Structures of each respective sorbent group are shown for reference.

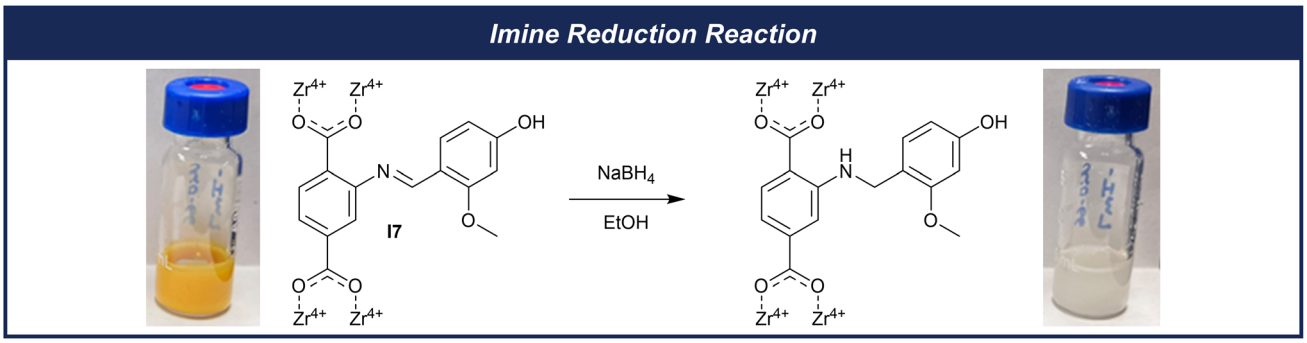

Fig. 6 Scheme for the reduction of imine-based MOF **I7** using sodium borohydride, and photographs of the MOF suspension before (left) and after (right) reduction.

lysis during digestion with a weak base, leading to recovery of the starting materials during NMR analysis.

In addition to being used to investigate the nature of functionalization, the NMR spectra of the digested MOFs were also employed to quantify the degree of functionalization for each material (Table 1). Except for **I6** and **I7**, which contain electron-donating methoxy groups, most of the imide-functionalized MOFs showed low degrees of functionalization ranging from 2% to 6%. **I6** and **I7** showed higher degrees of functionalization around 20% (23% and 18%, respectively), possibly resulting from the electron rich nature of their substituents. By contrast, amide-functionalized MOFs showed much higher degrees of functionalization, typically around 50% relative to the available number of NH_2 groups in the MOF. Only **A2**, with the most electron deficient adsorbent group, showed significantly lower functionalization, although it was still in line with the most functionalized imine MOFs.

To investigate whether functionalization altered the crystal structure of the MOFs in any way, powder X-ray diffraction (pXRD) measurements were performed (Fig. S64–S66†). The powder patters of the functionalized MOFs exhibited broad features at similar diffraction angles to those of unmodified UiO-66-NH_2, which is expected since the added adsorbent groups should not alter the general structure of the underlying MOF. However, significant broadening of the diffraction peaks was observed, suggesting a decrease in crystallinity for the **I1–**

Table 1 Characterization data for the MOFs studied in this work, including UiO-66, UiO-66-NH_2, UiO-66-OH, **I1–I7**, and **A1–A6**

Sorbent	% Functionalized[a]	SA_{BET} [b] ($m^2\ g^{-1}$)	Uptake capacity[c] (mmol g^{-1})[d]	Normalized capacity[e] (μmol m^{-2})
UiO-66	—	1360 ± 30	0.123 ± 0.013	0.090 ± 0.010
UiO-66-NH_2	0	1080 ± 120	0.137 ± 0.068	0.126 ± 0.063
UiO-66-OH	—	310 ± 60	0.124 ± 0.016	0.401 ± 0.051
I1	5	420 ± 40	0.084 ± 0.003	0.199 ± 0.007
I2	5	640 ± 40	0.104 ± 0.006	0.163 ± 0.009
I3	2	500 ± 50	0.315 ± 0.035	0.630 ± 0.070
I4	6	570 ± 10	0.144 ± 0.018	0.252 ± 0.032
I5	6	530 ± 20	0.109 ± 0.028	0.205 ± 0.053
I6	23	640 ± 70	0.028 ± 0.004	0.043 ± 0.006
I7	18	470 ± 40	0.144 ± 0.033	0.306 ± 0.071
A1	49	160 ± 20	0.055 ± 0.013	0.341 ± 0.079
A2	18	680 ± 20	0.058 ± 0.002	0.085 ± 0.003
A3	52	240 ± 90	0.075 ± 0.013	0.313 ± 0.053
A4	55	230 ± 10	0.049 ± 0.002	0.214 ± 0.010
A5	—[f]	470 ± 20	0.124 ± 0.003	0.264 ± 0.005
A6	65	140 ± 30	0.108 ± 0.041	0.769 ± 0.296

[a] Determined by ^{1}H NMR from the quantity of coupling partner incorporated relative to free NH_2-linker. [b] Brunauer–Emmett–Teller surface area determined by nitrogen gas adsorption at 77 K; measurements performed in triplicate. Samples were activated by drying overnight under vacuum at 200 °C. Thermal stability under these conditions was verified using thermogravimetric analysis (see ESI Fig. S67–S81†). [c] Uptake capacity for DMMP measured at 25 °C on samples dried in a vacuum oven at 120 °C; measurements performed in triplicate. [d] Uptake capacity reported as mmol of DMMP per gram of sorbent. [e] Normalized capacity refers to the uptake capacity divided by the surface area of the sorbent and is reported as μmol of DMMP per m^2 of the sorbent. [f] Percent of functionalization could not be obtained for **A5** due to the lack of observable protons for this coupling partner.

I7 and **A1–A6**. Similar results have been observed previously for poorly crystalline UiO-66 samples[43] as well as reactions of UiO-66 MOFs conducted in methanol, and it has been reported that this solvent can decrease MOF crystallinity by facilitating dissociation and exchange of the linkers from the zirconium nodes.[44] This interpretation is also in agreement with the decreased surface area measured of the functionalized materials. Therefore, it appears that the choice of solvent in this work is responsible for the broadened powder patterns observed here.

Nonetheless, we wondered whether the functionalized MOFs would exhibit porosity despite this loss of crystallinity. To answer this question, N_2 gas adsorption was used to measure the Brunauer–Emmett–Teller (BET) surface areas of the functionalized MOFs. In every case, a Type I isotherm was observed (Fig. S85–S97†), which is consistent with a microporous material.[45,46] Analysis of this data according to BET theory[45–48] following the Rouquerol criteria[49] yielded the surface areas shown in Table 1. Unsurprisingly, a broad, inverse correlation is observed between degree of functionalization and BET surface area, and all of the functionalized MOFs show decreased surface areas relative to unmodified UiO-66-NH_2 (Fig. 7). This observation is consistent with functionalization of the material, since the adsorbent groups are expected to consume some of the free volume within the MOF.

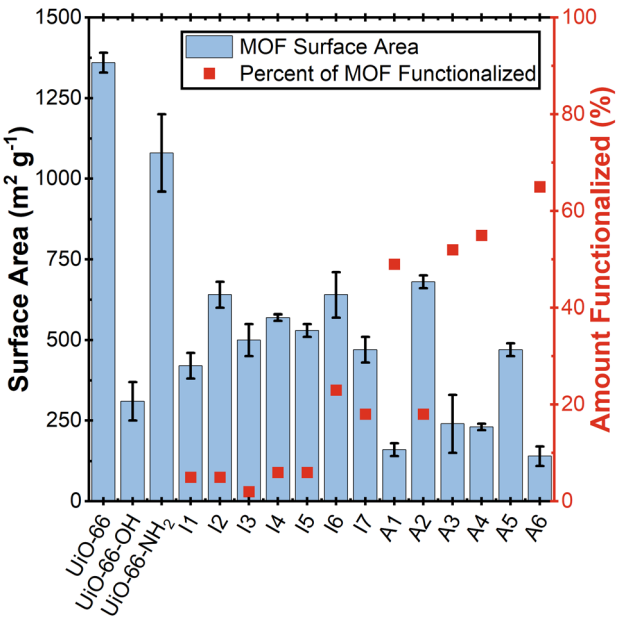

Fig. 7 Comparison of BET surface area (blue bars) relative to the degree of MOF functionalization (red squares). Error bars represent the standard deviation from three measurements.

The relationship between degree of functionalization and BET surface area is not perfectly linear, especially at lower degrees of functionalization where the impact on surface area is less consistent. In part, this observation may be due to the reduced crystallinity of the functionalized MOFs, which may decrease the porosity and therefore the surface area of the MOFs. In addition, defect sites likely contribute to this phenomenon in some way,[27] but exactly how the presence of such sites and their functionalization contribute to the measured surface areas is not clear.

To understand whether these materials might be suitable for gas adsorption applications, the surface areas of two common activated carbons were also measured by N_2 gas adsorption. Calgon BPL carbon, a commercial untreated activated carbon, exhibited a surface area of 1020 ± 40 m^2 g^{-1}. Instead, ASZM-TEDA impregnated carbon, an activated carbon treated with copper, silver, zinc, molybdenum, and triethylenediamine,[2] showed a lower surface area of 540 ± 60 m^2 g^{-1}, which is similar to many of the functionalized MOFs studied here. Therefore, it was concluded that while functionalization does lower the surface areas of the MOFs, these materials still possess suitable porosities for hazardous chemical adsorption applications. Nonetheless, future work can improve upon these measured surface areas by exploring the functionalization of MOFs with larger pores and higher surface areas prior to modification.

Finally, the functionalized MOFs were investigated as organophosphate adsorbents through a series of experiments employing a quartz crystal microbalance (QCM) testbed. A custom vapor generator was used to deliver chemical vapors to the QCM testbed, and the responses of QCM sensors coated with each functionalized MOF were monitored to quantify the amount of vapor adsorbed into the MOF. For each of the experiments described below, DMMP was selected as an organophosphate simulant based on literature precedence.[2–4,8,11,13,15,19] For full experimental details, see the ESI† Measurement of DMMP Uptake Capacity and Measurement of Henry's Law Binding Constants.

Experiments were first performed with a saturated DMMP vapor stream to interrogate the maximum uptake capacity of each MOF (Fig. 8, blue bars). In nearly every case, functionalized MOFs showed a decrease in uptake capacity for DMMP relative to unmodified UiO-66-NH_2. This result is not surprising considering the measured surface areas of these materials, which are all decreased relative to UiO-66-NH_2. In other words, since the free volume of the functionalized MOFs is reduced by functionalization, one can also expect the uptake capacities of the MOFs to decrease as well. Two notable exceptions are **I3** and **A6**, which show higher uptake capacities than unmodified UiO-66-NH_2 as well as UiO-66 and UiO-66-OH. In future work, the capacities of other functionalized MOFs could be improved by exploring MOFs with larger pores and higher surface area. However, in the present work, we wished to understand whether functionalization has *any* beneficial effect. Thus, the uptake capacities of the MOFs were normalized to surface area (Fig. 8, red bars), yielding more direct insight into the impact of the added sorbent groups. Interestingly, the normalized capacities of the MOFs suggest functionalization yields higher uptake capacity per unit of surface area, as most of the functionalized MOFs exhibit greater normalized capacities than unmodified UiO-66-NH_2.

To better understand how substituent electronics impact adsorbent performance, the normalized uptake capacities were analyzed relative to Hammett substituent constants, a series of constants used to quantify how electron rich or deficient different functional groups are. Hammett constants were originally developed to understand the ionization of benzoic acid derivatives,[50] but they have since been applied to understand reaction kinetics[51] and even non-covalent interactions.[52] In this work, correlation of the MOF normalized uptake capacities to Hammett substituent constants revealed two linear trends that provide insight into the impact of adsorbent

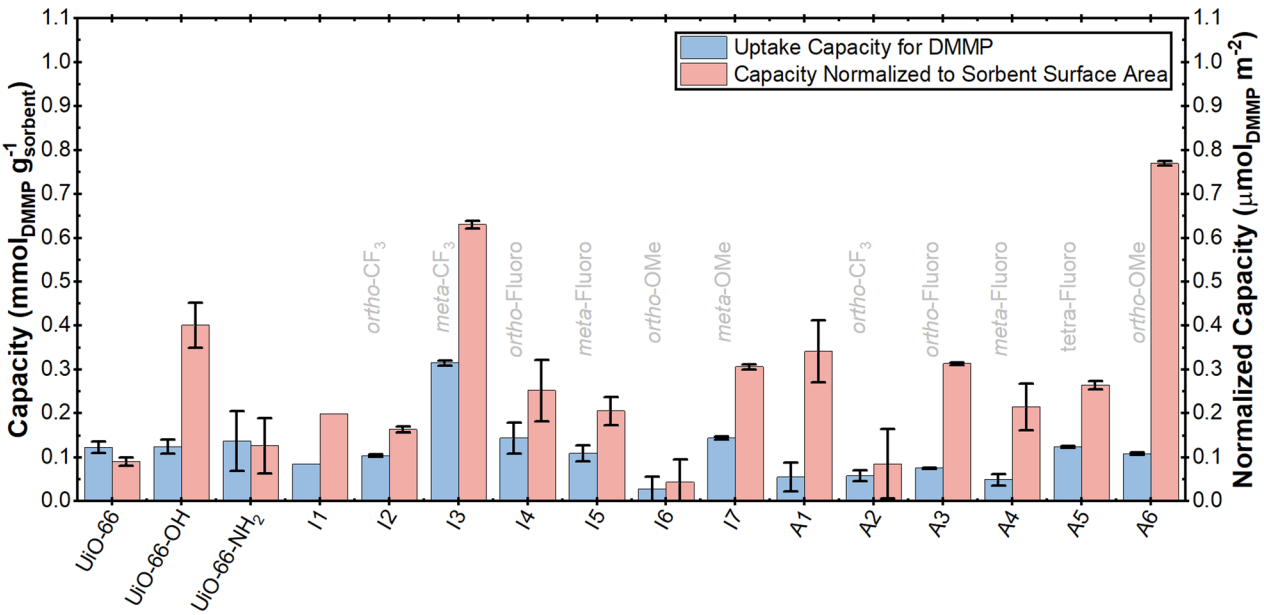

Fig. 8 Measurement of sorbent uptake capacity for DMMP using a QCM testbed. Capacity is displayed relative to sorbent weight (blue bars) and BET surface area (red bars). For samples in which functional groups are defined (light grey text), the positions noted are relative to the hydroxyl group.

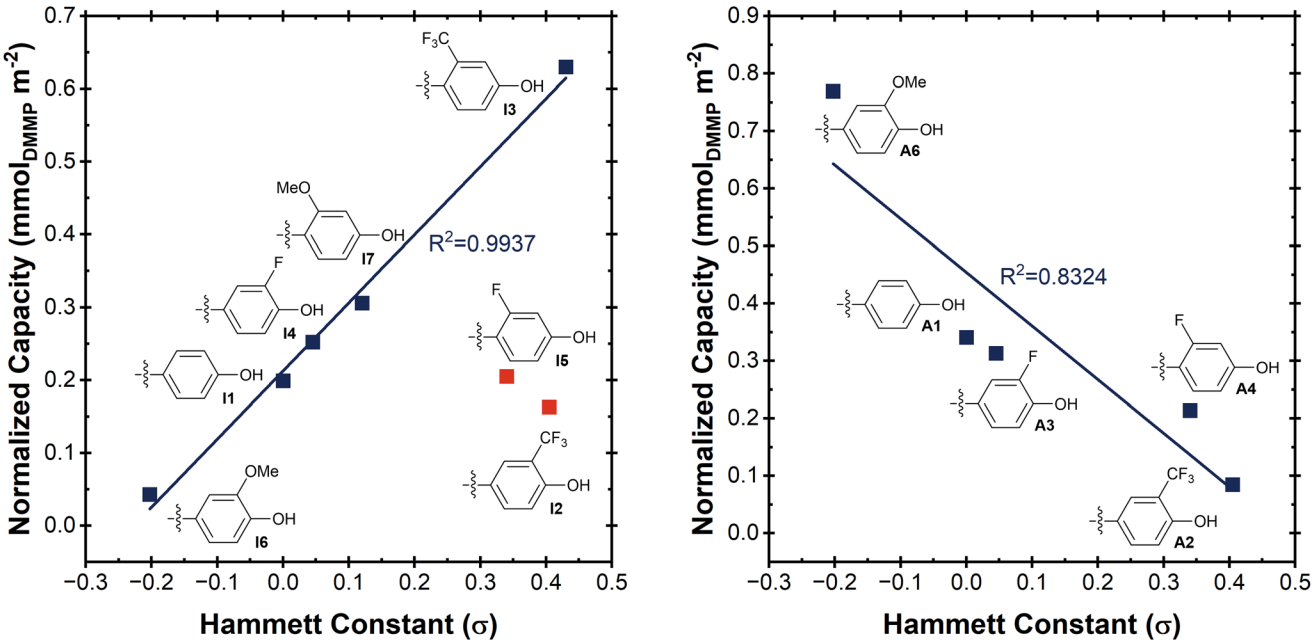

Fig. 9 Correlation of normalized sorbent capacity with Hammett constants for imine- (left) and amide-functionalized MOFs (right). Outliers that were omitted from the fit are displayed in red.

electronics on performance. In the case of imine-functionalized MOFs (Fig. 9, left), a positive trend is observed, which suggests electron-deficient groups are most beneficial to adsorbent uptake capacity. This observation is consistent with previous work,[15] although it should be noted that **I2** and **I5** are outliers in this trend. In the case of **I2**, sterics caused by the presence of a bulky CF_3 group adjacent to the hydroxyl binding site may explain the observed deviation. Often, Hammett constants are not considered for *ortho*-substituents, although they were estimated here as 0.75 of the value for the same substituent in the *para* position.[53]

By contrast, amide-functionalized MOFs exhibit a negative trend (Fig. 9, right), suggesting electron-rich adsorbent groups are most beneficial for high uptake capacity. It is surprising to find such a distinct difference between the imine- and amide-functionalized MOFs, and the cause for this difference remains unknown. Nonetheless, it appears that Hammett substituent constants provide a useful framework for understanding electronic effects within the adsorbent groups and predicting how different adsorbent groups may perform within a MOF.

Next, QCM experiments were performed with dilute DMMP vapor streams to measure Henry's law binding constants by comparing the [DMMP] adsorbed in the MOF relative to the [DMMP] in the headspace (Fig. 10, see ESI† – Measurement of Henry's law binding constants for full experimental details). All of the functionalized MOFs exhibit greater binding constants [log(K_H)] for DMMP than unmodified UiO-66-NH_2, supporting the benefit of functionalization with hydrogen-bond donating groups. In addition, a broad correlation between degree of functionalization and log(K_H) is observed, suggesting

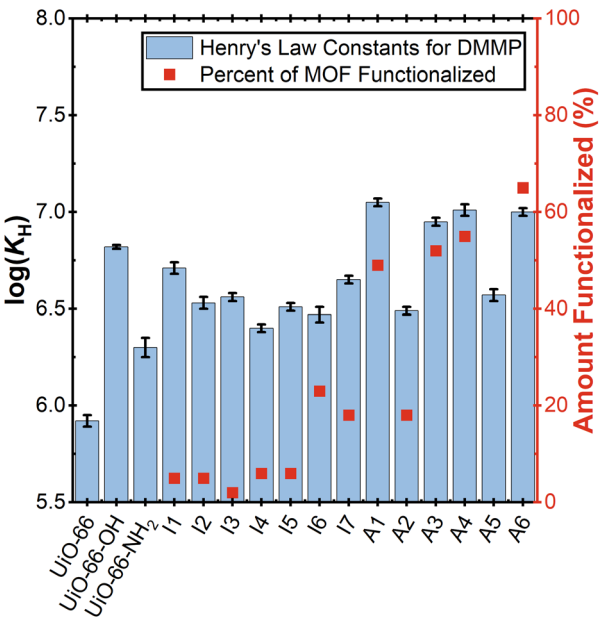

Fig. 10 Henry's law binding constants [log(K_H)] for imine- and amide-functionalized f-MOFs (blue bars) compared to the degree of MOF functionalization (red squares).

materials with more sorbent groups bind DMMP more strongly.

This correlation may be due to the existence of multiple binding sites, whose individual binding strengths are averaged in this measurement. Since this method is non-specific, it does not consider the possibility of multiple binding sites.

Table 2 Comparison of Henry's law binding constants for select sorbents with DMMP and toluene

Sample	Log(K_H) (DMMP)	Log(K_H) (toluene)	ΔLog(K_H)	ΔK_H
UiO-66-OH	6.82 ± 0.01	5.37 ± 0.03	1.45	28
UiO-66-NH_2	6.30 ± 0.05	4.95 ± 0.04	1.35	22
A6	7.00 ± 0.02	5.79 ± 0.03	1.21	16

While the functionalized MOFs have been designed to undergo binding through the added hydroxyl group, it is clear from the measurements of UiO-66 and UiO-66-NH_2 that other binding sites exist within the MOFs, although they do not bind DMMP as strongly as the added sorbent groups. Therefore, as the degree of functionalization increases, the average binding strength of the materials also increases. It is also interesting to note that several of the amide-functionalized MOFs (**A1**, **A3**, **A4**, and **A6**) show higher binding constants than UiO-66-OH, suggesting the hydroxyl groups within these MOFs bind DMMP more strongly than those in UiO-66-OH. However, the reason for this difference is unclear. It was suspected sorbent electronics might be a factor impacting these measured binding constants, but no clear trends were revealed through correlation to Hammett substituent constants.

To investigate how the adsorbent groups impact selectivity for DMMP, a final QCM experiment was performed to measure the Henry's law binding constant of several MOFs with toluene (Table 2). Interestingly, UiO-66-NH_2 shows greater selectivity for DMMP (~22× more affinity, as estimated by ΔK_H) than **A6** (~16× more affinity for DMMP than toluene), although lower affinity for both DMMP and toluene than **A6**. This result can be rationalized by considering that **A6** contains more binding sites for both DMMP (hydroxyl groups) and toluene (aromatic rings). Thus, while functionalization increases MOF affinity for DMMP, it also increases affinity for aromatic interferents such as toluene. In future work, this negative effect could be avoided by more careful selection of the adsorbent group, such as by addition of an aliphatic alcohol rather than an aromatic one. This approach is supported by the observation that UiO-66-OH is the most selective of the MOFs measured (~28× greater affinity for DMMP), since the hydroxyl groups in this MOF are directly attached to the linkers without any added aromatic groups.

Conclusion

Adsorbents for hydrogen-bond accepting chemicals such as organophosphates were developed by post-synthetic modification of UiO-66-NH_2. Using condensation reactions of benzaldehydes and benzoic acids, phenolic adsorbent groups were incorporated into the functionalized MOFs, along with additional methoxy, fluoro, and trifluoromethylphenyl groups to fine-tune adsorbent properties. For imine-functionalized MOFs in particular, characteristic color changes – and their disappearance upon imine reduction – provide support for successful functionalization.

When adsorbent performance was evaluated using an organophosphate simulant (DMMP), structure–property relationships were discovered showing that improvements in uptake capacity are correlated to sorbent electronics. For imine-functionalized MOFs, electron-deficient sorbent groups are most beneficial, while electron-rich groups provide the best results for amide-functionalized MOFs. The cause for this difference is not yet clear, but the use of Hammett substituent constants to elucidate these relationships has proven advantageous and should be considered in the future. In addition to the measurement adsorbent update capacity, experiments with DMMP yielded insight into the binding affinities of these sorbents and showed improvements in adsorbent affinity for DMMP due to functionalization. Materials with higher degrees of functionalization also showed the greatest improvements, highlighting the need for functionalization approaches with high conversion efficiencies.

Finally, preliminary experiments demonstrated how functionalization can be used to tune selectivity for target adsorbates over background, interferent chemicals. However, the added sorbent groups must be carefully selected to avoid unwanted interactions with interferents. Ongoing work seeks to incorporate these principles into subsequent sorbent design, as well as to address limitations of current sorbents by exploring MOFs with larger pores and greater surface areas.

Data availability

The data supporting this article have been included as part of the ESI.†

Conflicts of interest

The authors have no conflicts of interest to declare.

Acknowledgements

The authors would like to acknowledge the Office of Naval Research and the U.S. Naval Research Laboratory for funding this work. This project was supported in part by an appointment to the NRC Research Associateship Program at the U.S. Naval Research Laboratory in Washington, D.C., administered by the Fellowships Office of the National Academies of Sciences, Engineering, and Medicine. The authors would also like to acknowledge Courtney Roberts for discussions leading to early conceptions of this work; Thomas Sutto and Scott Mathews for assistance with X-ray diffraction studies; and Ken Grabowski for his support of this work.

References

1 M. A. R. Bhuiyan, L. Wang, A. Shaid, R. A. Shanks and J. Ding, Advances and applications of chemical protective clothing system, *J. Ind. Text.*, 2019, **49**, 97–138.

2 J. B. DeCoste and G. W. Peterson, Metal–organic frameworks for air purification of toxic chemicals, *Chem. Rev.*, 2014, **114**, 5695–5727.
3 M. Woellner, S. Hausdorf, N. Klein, P. Mueller, M. W. Smith and S. Kaskel, Adsorption and detection of hazardous trace gases by metal-organic frameworks, *Adv. Mater.*, 2018, **30**, 1704679.
4 T. Islamoglu, Z. Chen, M. C. Wasson, C. T. Buru, K. O. Kirlikovali, U. Afrin, M. R. Mian and O. K. Farha, Metal–organic frameworks against toxic chemicals, *Chem. Rev.*, 2020, **120**, 8130–8160.
5 C. Petit, C. Karwacki, G. Peterson and T. J. Bandosz, Interactions of ammonia with the surface of microporous carbon impregnated with transition metal chlorides, *J. Phys. Chem. C*, 2007, **111**, 12705–12714.
6 P. N. Brown, G. G. Jayson, G. Thompson and M. C. Wilkinson, Effect of ageing and moisture on the retention of hydrogen cyanide by impregnated activated charcoals, *Carbon*, 1989, **27**, 821–833.
7 J. G. O-Rear, J. R. Griffith and S. A. Reines, Some new fluorinated epoxies and polymeric derivatives, *J. Paint Technol.*, 1971, **43**, 113–119.
8 D. S. Ballantine, S. L. Rose, J. W. Grate and J. W. Wohltjen, Correlation of surface acoustic wave device coating responses with solubility properties and chemical structure using pattern recognition, *Anal. Chem.*, 1986, **58**, 3058–3066.
9 J. W. Grate, M. Klusty, R. A. McGill, M. H. Abraham, G. Whiting and J. Andonian-Haftvan, The predominant role of swelling-induced modulus changes of the sorbent phase in determining the responses of polymer-coated surface acoustic wave vapor sensors, *Anal. Chem.*, 1992, **64**, 610–624.
10 D. Rebière, C. Déjous, J. Pistré, J.-F. Lipskier and R. Planade, Synthesis and evaluation of fluoropolyol isomers as saw microsensor coatings: role of humidity and temperature, *Sens. Actuators, B*, 1998, **49**, 139–145.
11 R. A. McGill, V. K. Nguyen, R. Chung, R. E. Shaffer, D. DiLella, J. L. Stepnowski, T. E. Mlsna, D. L. Venezky and D. Dominguez, The "NRL-SAWRHINO": a nose for toxic gases, *Sens. Actuators, B*, 2000, **65**, 10–13.
12 R. A. McGill, T. E. Mlsna, R. Chung, V. K. Nguyen and J. Stepnowski, The design of functionalized silicone polymers for chemical sensor detection of nitroaromatic compounds, *Sens. Actuators, B*, 2000, **65**, 5–9.
13 B. A. Higgins, D. L. Simonson, E. J. Houser, J. G. Kohl and R. A. Mcgill, Synthesis and characterization of a hyperbranched hydrogen bond acidic carbosilane sorbent polymer: Carbosilane Sorbent Polymer, *J. Polym. Sci., Part A: Polym. Chem.*, 2010, **48**, 3000–3009.
14 C. A. Roberts and R. A. McGill, Bisphenol hypersorbents for enhanced detection of, or protection from, hazardous chemicals, *US Pat*, 11325100B2, 2022.
15 T. G. Grissom, C. A. Roberts, R. Rodrigues, M. R. Papantonakis, V. K. Nguyen and R. A. McGill, Sorbent interactions with hazardous chemicals and spectral detection strategies, in presented in part at *Chemical, Biological, Radiological, Nuclear, and Explosives (CBRNE) Sensing XXI*, Proc. SPIE 11416, Online Only, April, 2020.
16 N. S. Bobbitt, M. L. Mendonca, A. J. Howarth, T. Islamoglu, J. T. Hupp, O. K. Farha and R. Q. Snurr, Metal–organic frameworks for the removal of toxic industrial chemicals and chemical warfare agents, *Chem. Soc. Rev.*, 2017, **46**, 3357–3385.
17 D. W. Kang, S. E. Ju, D. W. Kim, M. Kang, H. Kim and C. S. Hong, Emerging porous materials and their composites for NH_3 gas removal, *Adv. Sci.*, 2020, **7**, 2002142.
18 Y. Liu, A. J. Howarth, N. A. Vermeulen, S.-Y. Moon, J. T. Hupp and O. K. Farha, Catalytic degradation of chemical warfare agents and their simulants by metal-organic frameworks, *Coord. Chem. Rev.*, 2017, **346**, 101–111.
19 Z. Ni, J. P. Jerrell, K. R. Cadwallader and R. I. Masel, Metal–organic frameworks as adsorbents for trapping and preconcentration of organic phosphonates, *Anal. Chem.*, 2007, **79**, 1290–1293.
20 D. Britt, D. Tranchemontagne and O. M. Yaghi, Metal-organic frameworks with high capacity and selectivity for harmful gases, *Proc. Natl. Acad. Sci. U. S. A.*, 2008, **105**, 11623–11627.
21 C. Montoro, F. Linares, E. Quartapelle Procopio, I. Senkovska, S. Kaskel, S. Galli, N. Masciocchi, E. Barea and J. A. R. Navarro, Capture of nerve agents and mustard gas analogues by hydrophobic robust MOF-5 type metal–organic frameworks, *J. Am. Chem. Soc.*, 2011, **133**, 11888–11891.
22 P. Z. Moghadam, D. Fairen-Jimenez and R. Q. Snurr, Efficient identification of hydrophobic MOFs: application in the capture of toxic industrial chemicals, *J. Mater. Chem. A*, 2016, **4**, 529–536.
23 I. Matito-Martos, P. Z. Moghadam, A. Li, V. Colombo, J. A. R. Navarro, S. Calero and D. Fairen-Jimenez, Discovery of an optimal porous crystalline material for the capture of chemical warfare agents, *Chem. Mater.*, 2018, **30**, 4571–4579.
24 I. Stassen, B. Bueken, H. Reinsch, J. F. M. Oudenhoven, D. Wouters, J. Hajek, V. Van Speybroeck, N. Stock, P. M. Vereecken, R. Van Schaijk, D. De Vos and R. Ameloot, Towards metal–organic framework based field effect chemical sensors: UiO-66-NH_2 for nerve agent detection, *Chem. Sci.*, 2016, **7**, 5827–5832.
25 S. Cai, W. Li, P. Xu, X. Xia, H. Yu, S. Zhang and X. Li, *In situ* construction of metal–organic framework (MOF) UiO-66 film on Parylene-patterned resonant microcantilever for trace organophosphorus molecules detection, *Analyst*, 2019, **144**, 3729–3735.
26 J. H. Cavka, S. Jakobsen, U. Olsbye, N. Guillou, C. Lamberti, S. Bordiga and K. P. Lillerud, A new zirconium inorganic building brick forming metal organic frameworks with exceptional stability, *J. Am. Chem. Soc.*, 2008, **130**, 13850–13851.
27 M. J. Katz, Z. J. Brown, Y. J. Colón, P. W. Siu, K. A. Scheidt, R. Q. Snurr, J. T. Hupp and O. K. Farha, A facile synthesis

of UiO-66, UiO-67 and their derivatives, *Chem. Commun.*, 2013, **49**, 9449.
28 M. J. Ingleson, J. P. Barrio, J.-B. Guilbaud, Y. Z. Khimyak and M. J. Rosseinsky, Framework functionalisation triggers metal complex binding, *Chem. Commun.*, 2008, 2680.
29 C. J. Doonan, W. Morris, H. Furukawa and O. M. Yaghi, Isoreticular metalation of metal–organic frameworks, *J. Am. Chem. Soc.*, 2009, **131**, 9492–9493.
30 J. S. Costa, P. Gamez, C. A. Black, O. Roubeau, S. J. Teat and J. Reedijk, Chemical modification of a bridging ligand inside a metal–organic framework while maintaining the 3D structure, *Eur. J. Inorg. Chem.*, 2008, **2008**, 1551–1554.
31 J. Chu, F.-S. Ke, Y. Wang, X. Feng, W. Chen, X. Ai, H. Yang and Y. Cao, Facile and reversible digestion and regeneration of zirconium-based metal-organic frameworks, *Commun. Chem.*, 2020, **3**, 5.
32 Z. Wang, K. K. Tanabe and S. M. Cohen, Accessing postsynthetic modification in a series of metal-organic frameworks and the influence of framework topology on reactivity, *Inorg. Chem.*, 2009, **48**, 296–306.
33 K. K. Tanabe and S. M. Cohen, Postsynthetic modification of metal–organic frameworks—a progress report, *Chem. Soc. Rev.*, 2011, **40**, 498–519.
34 S. M. Cohen, Postsynthetic methods for the functionalization of metal–organic frameworks, *Chem. Rev.*, 2012, **112**, 970–1000.
35 K. K. Tanabe and S. M. Cohen, Engineering a metal-organic framework catalyst by using postsynthetic modification, *Angew. Chem., Int. Ed.*, 2009, **48**, 7424–7427.
36 C. Volkringer and S. M. Cohen, Generating reactive MILs: isocyanate- and isothiocyanate-bearing MILs through postsynthetic modification, *Angew. Chem., Int. Ed.*, 2010, **49**, 4644–4648.
37 M. Kandiah, S. Usseglio, S. Svelle, U. Olsbye, K. P. Lillerud and M. Tilset, Post-synthetic modification of the metal–organic framework compound UiO-66, *J. Mater. Chem.*, 2010, **20**, 9848.
38 S. J. Garibay and S. M. Cohen, Isoreticular synthesis and modification of frameworks with the UiO-66 topology, *Chem. Commun.*, 2010, **46**, 7700.
39 X. Zhang, T. Xia, K. Jiang, Y. Cui, Y. Yang and G. Qian, Highly sensitive and selective detection of mercury(II) based on a zirconium metal-organic framework in aqueous media, *J. Solid State Chem.*, 2017, **253**, 277–281.
40 R. S. Brown, A. J. Bennet and H. Slebocka-Tilk, Recent perspectives concerning the mechanism of H_3O^+- and hydroxide-promoted amide hydrolysis, *Acc. Chem. Res.*, 1992, **25**, 481–488.
41 E. H. Cordes and W. P. Jencks, The mechanism of hydrolysis of schiff bases derived from aliphatic amines, *J. Am. Chem. Soc.*, 1963, **85**, 2843–2848.
42 Z. M. Soilis, T. H. Choi, J. Brennan, R. R. Frontiera, J. K. Johnson and N. L. Rosi, Ligand chromophore modification approach for predictive incremental tuning of metal–organic framework color, *Chem. Mater.*, 2023, **35**, 7741–7749.
43 M. Kim, J. F. Cahill, Y. Su, K. A. Prather and S. M. Cohen, Postsynthetic ligand exchange as a route to functionalization of 'inert' metal-organic frameworks, *Chem. Sci.*, 2012, **3**, 126–130.
44 J. Marreiros, C. Caratelli, J. Hajek, A. Krajnc, G. Fleury, B. Bueken, D. E. De Vos, G. Mali, M. B. J. Roeffaers, V. Van Speybroeck and R. Ameloot, Active role of methanol in post-synthetic linker exchange in the metal–organic framework UiO-66, *Chem. Mater.*, 2019, **31**, 1359–1369.
45 M. Thommes, K. Kaneko, A. V. Neimark, J. P. Olivier, F. Rodriguez-Reinoso, J. Rouquerol and K. S. W. Sing, Physisorption of gases, with special reference to the evaluation of surface area and pore size distribution (IUPAC Technical Report), *Pure Appl. Chem.*, 2015, **87**, 1051–1069.
46 J. Lykiema, K. S. W. Sing, J. Haber, M. Kerker, E. Wolfram, J. H. Block, N. V. Churaev, D. H. Everett, R. S. Hansen, R. A. W. Haul, J. W. Hightower and R. J. Hunter, Reporting physisorption data for gas/solid systems with special reference to the determination of surface area and porosity, *Pure Appl. Chem.*, 1985, **57**, 603–619.
47 S. Brunauer, P. H. Emmett and E. Teller, Adsorption of gases in multimolecular layers, *J. Am. Chem. Soc.*, 1938, **60**, 309–319.
48 K. S. Walton and R. Q. Snurr, Applicability of the BET method for determining surface areas of microporous metal–organic frameworks, *J. Am. Chem. Soc.*, 2007, **129**, 8552–8556.
49 J. Rouquerol, P. Llewellyn and F. Rouquerol, Is the BET equation applicable to microporous adsorbents?, in *Studies in Surface Science and Catalysis*, Elsevier, 2007, vol. 160, pp. 49–56.
50 L. P. Hammett, The effect of structure upon the reactions of organic compounds: benzene derivatives, *J. Am. Chem. Soc.*, 1937, **59**, 96–103.
51 C. Hansch, A. Leo and R. W. Taft, A survey of Hammett substituent constants and resonance and field parameters, *Chem. Rev.*, 1991, **91**, 165–195.
52 M. Lewis, C. Bagwill, L. K. E. Hardebeck and S. Wireduaah, The use of Hammett constants to understand the non-covalent binding of aromatics, *Comput. Struct. Biotechnol. J.*, 2012, **1**, e201204004.
53 M. Charton, The application of the Hammett equation to ortho-substituted benzene reaction series, *Can. J. Chem.*, 1960, **38**, 2493–2499.